

Solvent Density Dependence of Translational Diffusion of Transient Radicals in the Medium-Density Region of Trifluoromethane and Carbon Dioxide

Y. Kimura,* D. Kanda, M. Terazima, and N. Hirota*

Department of Chemistry, Graduate School of Science, Kyoto University, Kyoto 606-01, Japan

Received: December 16, 1996; In Final Form: April 4, 1997[®]

Translational diffusion constants of transient radicals produced by photochemical reactions of pyrazine, α -naphthoquinone, quinoxaline, and benzophenone with triethylamine (TEA) have been measured in trifluoromethane from $\rho_r = 1.4$ to 2.0, and α -naphthoquinone with TEA in carbon dioxide from $\rho_r = 1.2$ to 1.93, where ρ_r is the reduced density by the critical density of the solvent. The diffusion constants of the transient radicals almost linearly depend on the reciprocal of the solvent viscosity in the measured density region. The diffusion constants of the radicals are relatively smaller than those of stable molecules of similar molecular sizes, and the difference becomes smaller with increasing the molecular size, as is observed in liquid solution. However, the difference is smaller than that observed in the liquid solvent, which suggests that the effect of the solute-solvent attractive interaction on the diffusion constant is smaller in fluids at the medium-density region than in liquids.

1. Introduction

In recent years, a novel technique for measuring the diffusion constants of transient species has been developed by using the transient-grating (TG) spectroscopy.^{1–4} The studies using this technique have revealed very curious behavior of the translational diffusion constants of transient radicals in liquid solvents, i.e., the diffusion constants of transient radicals produced by the hydrogen abstraction reactions are much smaller than those of the parent molecules. For example, the diffusion constant of the ketyl radical of benzophenone (BP) produced by the reaction in 2-propanol is $0.33 \times 10^{-9} \text{ m}^2 \text{ s}^{-1}$, while the diffusion constant of BP in 2-propanol is $0.68 \times 10^{-9} \text{ m}^2 \text{ s}^{-1}$ at room temperature.² Several interesting aspects of the slow diffusion of transient radicals have been revealed; firstly, the smaller the molecular size of the radical is, the greater is the difference of the diffusion constant between the transient radical and the parent molecule.³ Secondly, the activation energy of the diffusion constant of the transient radical is larger than that of the parent molecule.⁴ These experimental results are well simulated by a model in which the effective volume of the radical is larger than that of the parent molecule.^{3,4} The large effective volume is often explained by the specific interaction between the solute and the solvent molecules as in the case of the slow diffusion of ions.⁵ Very recently, however, it was found that the benzyl radical produced by the photodissociation of dibenzylketone does not show the slow diffusion in contrast to the case of the ketyl radical.⁶ This difference of the diffusion constant may be ascribed to the electronic character of the radical molecule. Ab initio molecular orbital calculations have revealed a very unique electronic character of the transient radicals: the response of intramolecular charge polarization by an external electrostatic field is much larger in the radicals, such as pyrazinyl radical and benzophenone ketyl radical, than in their parent molecules.⁷ This means that the radicals are very polarizable due to the electrostatic field by the solvent molecule, which may bring in a strong solute-solvent attractive interaction.

It is an interesting issue to study the diffusion of the transient radicals in fluids in the medium-density region near the gas-

liquid critical density. In the medium-density region, it is well-known that the attractive interaction between molecules plays a dominant role in determining structures than in the liquid at high densities and that molecular association is much enhanced.^{8,9} However it is not clear how this attractive interaction appears in the dynamic properties of the solute molecule. In recent years there have been a lot of data accumulated for the translational diffusion constants of stable organic molecules in fluids in the medium-density region, that is, supercritical fluids, especially for carbon dioxide.¹⁰ These studies have shown several interesting aspects of the diffusion in the medium-density region. Firstly, the diffusion constants of aliphatic esters and ketones are proportional to the reciprocal of the solvent viscosity,^{11,12} while aromatic molecules, such as benzene (BZ) and naphthalene (NP), are not.¹³ Secondly, there holds a good power law between the diffusion constant and the molal volume at the boiling point, when compared at the constant temperature and pressure.^{14,15} These relations are, however, still empirical. The study of the diffusion constants of the transient radicals experiencing strong solute-solvent attractive interactions may clarify how the attractive interaction plays a role in the diffusion process in the medium-density region.

In the present work, we have studied the diffusion constants of the transient radicals in trifluoromethane (CF_3H) and carbon dioxide (CO_2). We have chosen various sizes of parent molecules: pyrazine (PR), α -naphthoquinone (NQ), quinoxaline (QX), and benzophenone (BP). Upon photoexcitation, these molecules undergo hydrogen abstraction reactions if appropriate hydrogen donors exist. Since they cannot abstract hydrogen from the solvent molecules under study (CF_3H and CO_2), we have added a small amount of triethylamine (TEA). The diffusion constants of the radicals produced by the photochemical reactions with TEA have been measured by the TG method. We have covered the density region from $\rho_r = 1.2$ to 2.0, where ρ_r is the reduced density defined by the ratio to the critical density of the solvent. The density region studied corresponds to the intermediate region which connects the gaseous ($\rho_r \approx 0$) to the liquid densities ($\rho_r \approx 2.7$). In this density region, we have also observed the slow diffusion of the transient radicals compared with stable molecules of similar sizes.

[®] Abstract published in *Advance ACS Abstracts*, May 15, 1997.

2. Experimental Section

The experimental setup for measuring the diffusion constants of the transient radicals by the TG method under high pressure is given elsewhere.¹⁶ We briefly describe the essential step for the measurement. An excimer laser (Lumonics Hyper 400) ($\lambda_{\text{ex}} = 308$ nm) was used for the photoexcitation in CF_3H and CO_2 . Typically the excitation laser power for the TG measurement was less than 0.1 mJ/pulse. After crossing two pump beams from the excimer laser in a sample solution, the time dependence of the grating probed by a He-Ne laser ($\lambda_{\text{pr}} = 633$ nm) was monitored with a photomultiplier (Hamamatsu R928). The repetition rate of the excitation pulse was typically 4 Hz.

The high-pressure optical cell used for the measurement was described previously.¹⁷ The solution in the cell was stirred by a magnetic stirrer to prevent the accumulation of the photochemical product in the irradiation region. The temperature was kept within ± 0.1 K by circulating the thermostated water through the cell, and the pressure of the cell was measured by a strain gage (Kyowa PGM 500 KH) within ± 0.02 MPa. The densities of the fluids were calculated by empirical equations of states.^{18,19} The concentration of the solute was less than 3×10^{-3} mol dm^{-3} , and the concentration of TEA added as a hydrogen donor was ca. 6×10^{-2} mol dm^{-3} . The effect of the solute on the PVT of the solvent was neglected.

The photochemical reaction in CF_3H has also been measured by the standard nanosecond transient absorption method. The transient absorption was measured at a 90° angle with pump (excimer laser) and the probe beams. A Xe flash lamp (Eagel Technology YXP-150RE) was used as a source of the probe beam. The timing between the pump and the probe beams was tuned by an delay generator (EG&G, 9650), and the transient absorption was monitored by a photo multiplier tube (Hamamatsu Photonics R446) attached to a spectrometer (Engis Model 600). The high-pressure optical cell with three quartz windows used for the measurement has been described elsewhere.²⁰

CF_3H (Ashahi Glass, >99.999%) and CO_2 (Sumitomo Seika, > 99.99%) were used as received. TEA and 1,4-cyclohexadiene (CHD), QX (Nacalai Tesque) were used without further purification. NQ, PR, and BP (Nacalai Tesque) were purified by recrystallization from ethanol before use.

3. Results

Figure 1 shows typical TG signals at $\rho_r = 1.80$ and 323.2 K in CF_3H . We have obtained similar signals for sample solutions under study. The time profile of the TG signal shows a complex feature, which is due to the fact that the TG signal (I_{TG}) is proportional to the squares of the peak-null difference of the refractive index (Δn) and the absorption coefficient (Δk) created by the photoexcitation as follows:

$$I_{\text{TG}} \propto (\Delta n)^2 + (\Delta k)^2 \quad (1)$$

There are mainly two possible origins which create the refractive index change: the thermal grating and the species grating. The thermal grating derives from the expansion of the solvent due to the heat released by the photochemical processes, which decreases the refractive index at the hot fringe. The signal decays with the thermal diffusion across the grating fringe. The species grating derives from the variation of the number of chemical species by the photochemical reaction, which decays the mass transport across the grating fringe and plausible chemical reactions. In general, the TG signal is expressed by these two contributions in the following way:²

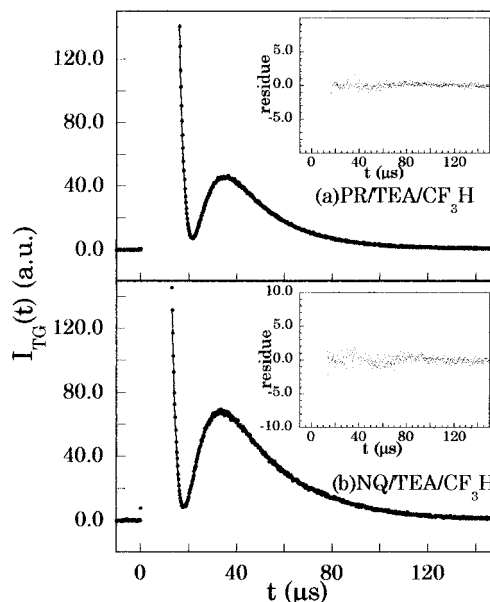


Figure 1. Typical transient grating signals observed for (a) PR and (b) NQ with TEA in CF_3H at $\rho_r = 1.80$ and 323.2 K, for $q^2 =$ (a) $2.90 \mu\text{m}^{-2}$ and (b) $2.89 \mu\text{m}^{-2}$, respectively. The figures inserted show the residual for the fit by eq 3 with $\tau_1 =$ (a) $6.71 \mu\text{s}$ and (b) $6.91 \mu\text{s}$, and $\tau_2 =$ (a) $37.6 \mu\text{s}$ and (d) $49.2 \mu\text{s}$, respectively.

$$I_{\text{TG}}(t) \propto$$

$$\begin{aligned} & \{ \Delta n_{\text{th}} \exp(-D_{\text{th}} q^2 t) + \sum_r \Delta n_r \exp[-(D_r q^2 + k_r) t] + \\ & \sum_p \Delta n_p \exp(-D_p q^2 t) \}^2 + \{ \sum_r \Delta k_r \exp[-(D_r q^2 + k_r) t] + \\ & \sum_p \Delta k_p \exp(-D_p q^2 t) \}^2 \quad (2) \end{aligned}$$

where Δn_{th} , Δn_r , Δn_p are the peak-null difference of the refractive index due to the thermal grating and the gratings of the radical and the parent molecules, respectively. Δk_r and Δk_p are the peak-null difference of the absorption coefficients due to the gratings of the radical and the parent molecules. D_{th} , D_r , and D_p are the thermal diffusion constant and the diffusion constants of the radical and of the parent molecule, respectively. q is the grating lattice vector, and k_r denotes the decay constant of the peak-null difference of the radical due to nondiffusive process. In the liquid solution, the thermal diffusion is much faster than the mass transport, and the TG signal from the species grating was analyzed well separated from the thermal signal. In the case of BP with TEA in liquid solution, the TG signal due to the species grating was analyzed from the contributions of the ketyl radical of BP and the parent BP, and the signals due to TEA and its derivative have not been well identified probably due to its low absorbance near the probe wavelength (633 nm). Furthermore, in practice, k_r can be neglected in the liquid solvent, which suggests that the lifetime of the radical is much longer than the diffusion process over the grating lattice. In the present case, all signals in CF_3H and CO_2 are well simulated by the following function:

$$I_{\text{TG}} \propto |A_1 \exp(-t/\tau_1) - A_2 \exp(-t/\tau_2)|^2 + |B_2 \exp(-t/\tau_2)|^2 \quad (3)$$

where A_1 , A_2 , B_2 , τ_1 , and τ_2 are the positive constants, and $\tau_1 < \tau_2$. The inset figures in Figure 1 are the residual for the fit by eq 3. The first term in eq 3 corresponds to the change of the refractive index, and the second term corresponds to the change of the absorption coefficient. In our study, B_2 was much smaller

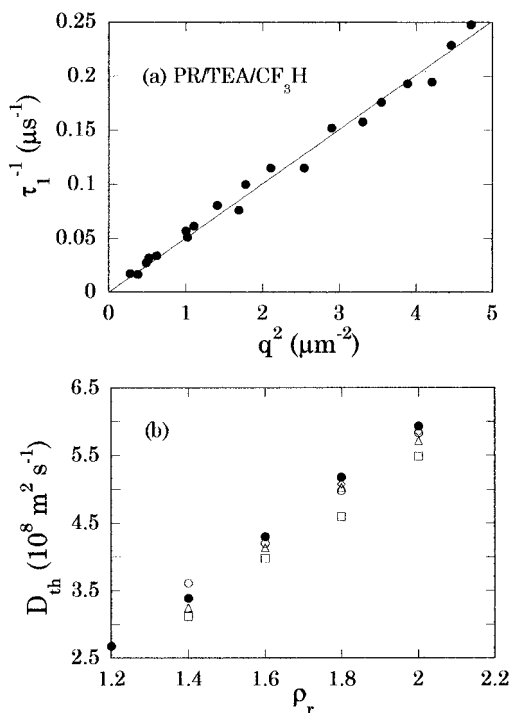


Figure 2. (a) The dependence of the decay constants ($1/\tau_1$) due to the thermal grating on q^2 for PR with TEA in CF₃H at $\rho_r = 1.80$ and 323.2 K. (b) The solvent density dependence of the thermal diffusion constant obtained by the slope of the each plot for CF₃H at 323.2 K: Δ , PR; \diamond , QX; \square , BP; \square , NQ; \bullet , calculated values by $\lambda/\rho C_p$.

than A_2 . We ascribe the first component of the signal (τ_1) to the thermal grating, and the slower component (τ_2) to the species grating due to the radical produced by the reaction, because of the order of decay time τ_1 and τ_2 and of the signs of A_1 and A_2 . The reason is as follows: since the absorption spectra of the parent molecules and the radicals under study lie in the blue-shifted wavelength region to the probe wavelength, the molecular refractive index is positive at the probe wavelength because of the Kramers-Kronig relation. Therefore, the molecular refractive index of the parent molecule contributes to the TG signal with the same phase as the thermal grating and that of the radical with the opposite phase. The positive values of A_1 and A_2 mean that the signal due to the mass grating is from the radical and not from the parent molecule. In general, the absorption of the radical is red shifted to the parent molecule, and the absorption of the parent molecule in the medium-density region is slightly blue shifted to the spectrum in liquid. This explains the reason why only the signal due to the radical is observed.

Figure 2a shows a typical plot of the decay constants ($1/\tau_1$) due to the thermal grating obtained by the fit to eq 3 versus q^2 in the case of PR in CF₃H at $\rho_r = 1.80$ and 323.2 K. The plot is well simulated by a straight line which intercepts the origin, and the slope gives the thermal diffusion constant of the solvent fluid multiplied by q^2 . As is shown in Figure 2b, the thermal diffusion constant obtained by this method coincides with the value obtained by the calculation from the relation $D_{\text{th}} = \lambda/\rho C_p$, where λ is the thermal conductivity and C_p is the heat capacity at the constant pressure.

Figure 3 shows the plot of the decay constants ($1/\tau_2$) due to the species grating of the radicals at $\rho_r = 1.80$ and 323.2 K, and each plot gives a straight line. In the case of BP and NQ we obtained much better fits with small positive values of the intercepts. This implies that in these cases the radicals have limited lifetimes within the diffusion process. The value of k_r is dependent on the solvent density, and we could fit the result

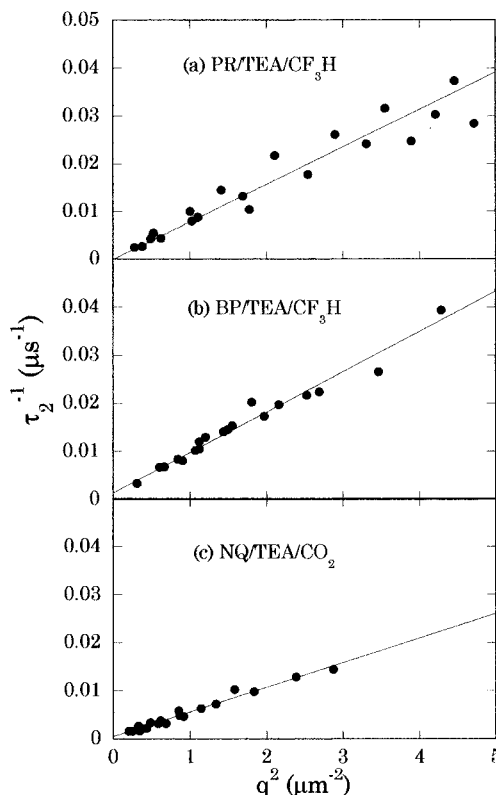


Figure 3. The dependence of the decay constants ($1/\tau_2$) due to the species grating on q^2 for (a) PR, (b) BP with TEA in CF₃H, and (c) NQ with TEA in CO₂, at $\rho_r = 1.80$ and 323.2 K, respectively.

with $k_r = 0$ below $\rho_r = 1.6$. The values are $1.4 \times 10^3 \text{ s}^{-1}$ for BP and $1.2 \times 10^3 \text{ s}^{-1}$ for NQ in CF₃H at $\rho_r = 1.80$.

To ensure the photochemical reaction, we have measured the transient absorption spectra. Figure 4a shows the transient absorption spectra at several time delays after the photoexcitation of BP with TEA in CF₃H at $\rho_r = 2.0$ and 323.2 K. The absorption spectrum at 5 μs after the photoexcitation is quite similar to the spectra observed for the benzophenone ketyl radical (BP \cdot) in liquid solvents²¹ and in fluid ethane.²² The decay of the transient absorption signal monitored at 320 nm after the photoexcitation was simulated by the second-order decay. Using the value of the absorption coefficient of $1.8 \times 10^4 \text{ mol}^{-1} \text{ dm}^3 \text{ cm}^{-1}$,²¹ the second-order reaction coefficient is estimated as $1 \times 10^{10} \text{ mol}^{-1} \text{ dm}^3 \text{ s}^{-1}$. Considering that the decay constant of BP \cdot obtained by the TG signal in Figure 3 is on the order of $1 \times 10^3 \text{ s}^{-1}$, the concentration of BP \cdot in the TG measurement is estimated to be $10^{-7} \text{ mol dm}^{-3}$, which is slightly smaller than the previous estimation for the liquid phase reaction.² This is reasonable because the signal due to the species grating was weaker than that observed in liquid solution.

In the case of NQ with TEA, the situation is somewhat different. The photochemistry of NQ is complex depending on the solvent and the hydrogen donor. To clarify what happens in this system, we have measured the transient absorption spectra for the following three systems: NQ, NQ with 1,4-cyclohexadiene (CHD), and NQ with TEA in CF₃H. Figure 4b shows the transient absorption spectra for three systems above-mentioned at $\rho_r = 1.5$ and 323.2 K. In the case of pure NQ, the band around 360 nm was observed, which decays almost completely within a few microseconds. The shape of the spectrum is quite similar to that reported for the triplet state of NQ in acetonitrile.²³ With adding CHD, the transient absorption spectrum becomes double peaked, and the lifetime of the signal becomes longer. This band can be assigned to the band due to the radical produced by the hydrogen abstraction reaction (NQ \cdot),

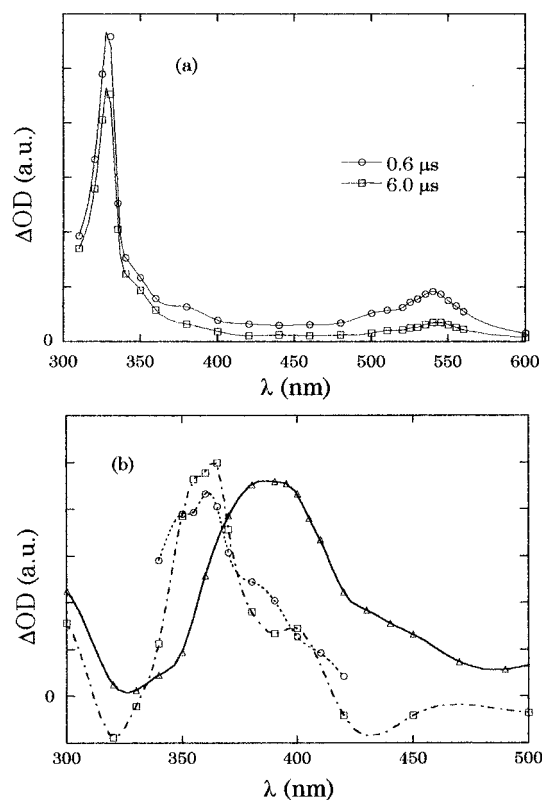


Figure 4. Transient absorption spectra at several delay times after the photoexcitation: (a) BP with TEA in CF_3H at $\rho_r = 2.0$ and 323.2 K, (b) NQ (0.1 μs , \circ), NQ with CHD (0.4 μs , \square), NQ with TEA (0.3 μs , \triangle), in CF_3H , at $\rho_r = 1.5$ and 323.2 K, respectively. The delay time to the photoexcitation is denoted in the parentheses.

as in ref 23. The absorption spectrum of NQ with TEA shows it becoming broadened, red shifted, and structureless. This absorption is very similar to that observed for the radical anion ($\text{NQ}^{\bullet-}$) in water.²⁴ The decay constant also becomes longer than that of NQ^{\bullet} . The different photochemical reactions between TEA and CHD are due to the difference of the ionization potential of the donor molecules. We have also observed similar transient absorption spectra for NQ, NQ with CHD, and NQ with TEA both in liquid benzene and chloroform. This leads to the conclusion that a photochemical reaction occurring in CO_2 is similar to that in CF_3H . It is not certain how an anion radical is stable during the TG measurement even in a nonpolar solvent, but a possible explanation is that $\text{NQ}^{\bullet-}$ makes a stable molecular complex with nongeminate TEA. The complex formation will also be reflected on the diffusion constant as is discussed below.

4. Discussion

Table 1 summarizes the diffusion constants of the transient radicals obtained in this study. We abbreviate the radicals produced by the hydrogen abstraction reactions of PR and QX as PR^{\bullet} and QX^{\bullet} , respectively. As is mentioned in the introduction, there is no universal good equation which explains the density dependence of the diffusion constant in the medium-density region. The dynamic quantity of the solvent which is used most frequently to correlate the diffusion constant is the viscosity. The most well-known equation using the viscosity is the Stokes–Einstein relation which is expressed as

$$D = \frac{kT}{6\pi\eta R} \quad (4)$$

where k is the Boltzmann constant, η is the solvent viscosity,

TABLE 1: Diffusion Constants (D_r) of Transient Radicals Produced by Photochemical Reactions with TEA in CF_3H (and CO_2) at 323.2 K

ρ_r	D_r^a				
	PR^{\bullet}	QX^{\bullet}	$\text{NQ}^{\bullet-}$	$\text{NQ}^{\bullet-}/\text{CO}_2$	BP^{\bullet}
1.20				0.92 ± 0.08	
1.40	1.03 ± 0.06		0.87 ± 0.05	0.82 ± 0.03	1.08 ± 0.08
1.60	0.98 ± 0.04		0.70 ± 0.04	0.66 ± 0.03	0.98 ± 0.03
1.80	0.78 ± 0.07	0.75 ± 0.09	0.60 ± 0.05	0.51 ± 0.05	0.84 ± 0.07
1.93				0.38 ± 0.07	
2.00	0.68 ± 0.04	0.67 ± 0.04	0.43 ± 0.06		0.73 ± 0.07

^a Unit of D_r is $10^{-8} \text{ m}^2 \text{ s}^{-1}$.

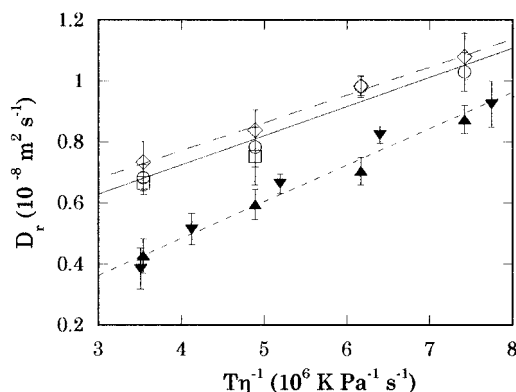


Figure 5. Solvent viscosity dependence of the diffusion constants of the radicals produced by the reaction with TEA in CF_3H (\circ , PR^{\bullet} ; \square , QX^{\bullet} ; \diamond , BP^{\bullet} ; \blacktriangle , $\text{NQ}^{\bullet-}$) and CO_2 (\blacktriangledown , $\text{NQ}^{\bullet-}$) at 323.2 K. The straight lines are those obtained by the least-squares fit to the data: solid line, PR^{\bullet} ; broken line, BP^{\bullet} ; dotted line, $\text{NQ}^{\bullet-}$.

and R is the radius of the solute molecule. We cannot use this relation to correlate the diffusion constants, since this relation does not hold for aromatic molecules in the supercritical fluid.¹³ A number of modified equations have been proposed to correlate the diffusion constant with the viscosity. One of the simplest and most successful equations is the following one:¹³

$$D = a_1(\eta/T)^{-b_1} \quad (5)$$

where a_1 and b_1 are the constants characteristic to the molecule. This equation is quite an empirical one, and we have to determine the parameter a_1 and b_1 from the experimental data.

Figure 5 shows the viscosity dependence of the diffusion constants of the transient radicals obtained by our experiment. As is shown in the figure, the diffusion constants are almost linearly dependent on the reciprocal of the solvent viscosity. It is interesting that the diffusion of the anion radical $\text{NQ}^{\bullet-}$ does not show meaningful polarity dependence, i.e., the diffusion constants in CF_3H and in CO_2 are very close. This is a similar situation observed for 1',3',3'-trimethyl-6-nitrospiro[2H-1-benzopyran-2,2'-indoline] (SP). In a previous study,²⁵ we have compared the diffusion constant of charge-separated SP in CO_2 with that in CF_3H . We have obtained the result that the diffusion constants are well scaled by the solvent viscosity and that they are not dependent on the solvent polarity. We ascribed the reason to the large molecular size. In the present case, if $\text{NQ}^{\bullet-}$ makes a complex with TEA, the molecular size becomes comparable to SP, which explains small solvent polarity effect on the diffusion constant.

Now we will discuss the slope in Figure 5. In the case of BP^{\bullet} and PR^{\bullet} , the fitted lines clearly do not intercept the origin, which indicates that the Stokes–Einstein relation does not hold. This is a similar tendency observed for aromatic molecules in the medium-density region.¹³ If we calculate the radius from

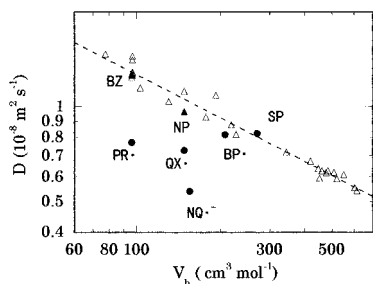


Figure 6. Plot of the diffusion constants (D) of various molecules in CO_2 at 16.0 MPa and 313.2 K versus their molal volumes at the boiling points. Open triangles are diffusion constants of stable organic molecules taken from refs. 13, 26–28. The diffusion constants of BZ and NP are indicated by the closed triangle.

the slope of the fit by modifying the Stokes–Einstein relation with including a constant term (the intercept of the linear fit), we obtain larger values of the molecular radius (0.76 nm for PR^* , 0.61 nm for NQ^{*-} , 0.80 nm for BP^*) in comparison with the values estimated from the van der Waals geometry (0.259 nm for PR^* , 0.319 nm for NQ^* , and 0.348 nm for BP^*).⁴ The data can also be fitted equally well by eq 5, but we could not find meaningful relation for the parameter a_1 and b_1 with molecular parameters [$a_1 = 0.32$ (PR^*), 0.11 (NQ^{*-}), 0.37 (BP^*), and $b_1 = 0.59$ (PR^*), 1.03 (NQ^{*-}), 0.53 (BP^*)].

As for the viscosity dependence of the diffusion constant, the transient radicals show a similar tendency to those of stable aromatic molecules. Next we compare the diffusion constants of the radicals with those of stable molecules of similar sizes. In the previous studies in solution,^{1–4} we could compare the diffusion constants of the radicals with the parent molecules since both of the diffusion constants could be measured simultaneously. In this study, however, the signal of the parent molecule could not be detected. Furthermore, if we want to compare the diffusion constants of the radicals with those of stable organic molecules in CF_3H , the comparison is difficult since not so many diffusion constants in CF_3H have been reported. Empirically it is known that there is a good correlation between the diffusion constant and the molal volume at the boiling point, when compared at the constant temperature and pressure in the case of CO_2 .^{14,15} Here we will follow this method and compare the diffusion constants of the radicals with stable organic molecules in CO_2 at 313.2 K and $\rho_r = 1.7$, where many data of the diffusion constants have been accumulated.^{13,26–28} The diffusion constants of the radicals for CO_2 at 313.2 K and $\rho_r = 1.7$ are estimated by the viscosity dependence of the diffusion constant, i.e., we have used the diffusion constant in CF_3H at the corresponding viscosity calculated by the viscosity dependence in Figure 5. The molal volumes at the boiling point of PR^* and QX^* are assumed to be the same as those of BZ ($96 \text{ cm}^3 \text{ mol}^{-1}$) and NP ($148 \text{ cm}^3 \text{ mol}^{-1}$).²⁹ The values of NQ^{*-} and BP^* are assumed to be the same as those for NQ ($155 \text{ cm}^3 \text{ mol}^{-1}$) and BP ($207 \text{ cm}^3 \text{ mol}^{-1}$), whose values are calculated by the method of LeBas.³⁰

Figure 6 shows the logarithmic plot of the diffusion constant versus the molal volume at the boiling point (V_b). The diffusion constants of the transient radicals are smaller than those of the stable molecules of similar sizes as observed in liquids, and the difference becomes smaller with increasing the molal volume of the radical. The relatively smaller value of NQ^{*-} may be ascribed to the complex formation. It is to be noted that the magnitude of the difference at this density is different from that observed in liquid solution. For the molecules under study, the ratios of the diffusion constant of the radical to the parent molecule is 0.25 for PR^* , 0.36 for QX^* , 0.31 for NQ^* , and 0.49 for BP^* in 2-propanol, respectively.³ In the fluid at this density,

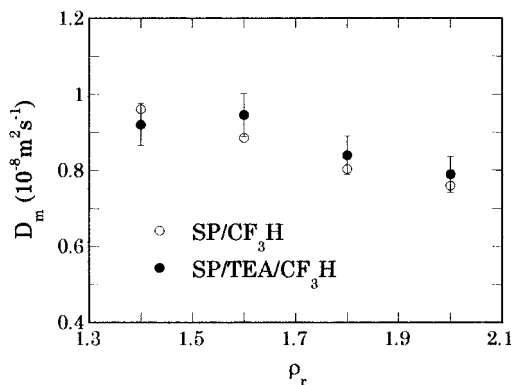


Figure 7. Density dependence of the diffusion constants of SP with and without TEA in CF_3H at 323.2 K.

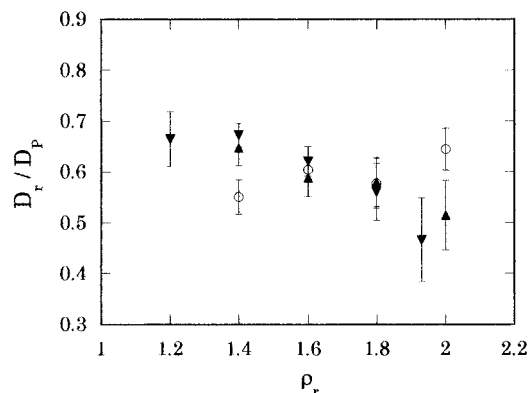


Figure 8. Density dependence of the ratios of the diffusion constants of the transient radicals (D_m) to those of stable molecules of similar molecular volumes (D_p): \circ , PR^* in $\text{CF}_3\text{H}/\text{BZ}$ in CO_2 ; \blacktriangle , NQ^* in $\text{CF}_3\text{H}/\text{NP}$ in CO_2 ; \blacktriangledown , NQ^{*-} in CO_2/NP in CO_2 .

the ratios are 0.60 for PR^* , 0.69 for QX^* , 0.52 for NQ^{*-} , and 0.90 for BP^* , respectively.

One possible origin of the slow diffusion of the radicals in fluids in the present study is the small amount of TEA added, i.e., the entrainer effect. In fact, several experimental studies of the entrainer effect on the diffusion constants indicate that the entrainer makes the diffusion process slow.³¹ To test the entrainer effect due to the small amount of TEA on the diffusion constant of the radicals, we have measured the diffusion constant of SP with TEA in CF_3H by the TG method. The concentration of TEA was the same as those for the study of the radical. Figure 7 shows the results. We could not detect a significant entrainer effect on the diffusion constant of the charge-separated state of SP over the density region in this study. This is understandable because the concentration of TEA is much smaller (ca. $1/10$) than the typical concentration of the studies on the entrainer effect.

It is an interesting issue how the relative value of the diffusion constant of the radical to that of the stable molecule of a similar size changes with the solvent density. We do not have so many data on the density dependence of the diffusion constant of aromatic molecules similar to those studied in this work, but the data on BZ and NP are available.^{14,32–35} Therefore, we have compared the diffusion constant of PR^* in CF_3H with BZ in CO_2 and of NQ^{*-} in CF_3H and CO_2 with NP in CO_2 at the corresponding viscosity. The comparison of NQ^{*-} with NP may not be rationalized, since we have mentioned the possibility of the complex formation. The calculated value should be considered to contain both effects of the complex formation and the difference of the strength of the attractive interactions. As is shown in the Figure 8, the ratio for PR^* is almost constant irrespective of the solvent density in the measured region within

errors. In the case of $\text{NQ}^{\bullet-}$, the ratio becomes somewhat smaller with increasing the solvent density. Considering that the reduced density of ordinary liquid is around 2.7, the ratio should decrease with increasing the solvent density, if the relatively large ratio compared with that in liquid (Figure 8) reflects the effect of the density and not the characteristics of CO_2 and CF_3H . In this sense, the behavior of $\text{NQ}^{\bullet-}$ is normal, and the ratio of PR^{\bullet} should decrease at the higher-density region. This means that the density region under study is not liquidlike from the view point of the effect of the attractive interaction on the diffusion, which makes a contrast to the case of the properties which reflect the structure of the fluid such as the partial molal volumes,³⁶ e.g., the partial molal volume of NP in CO_2 has a large negative value near the critical density of the solvent, but it becomes a positive value already around $\rho_r = 2.0$, as is observed in liquid solvent.

We can summarize the results of the radical diffusion in the medium-density region as follows: (a) the diffusion constant is almost linearly dependent on the reciprocal of the solvent viscosity in the measured density region, but is also fitted equally well by eq 5; (b) the diffusion constant of the radical is smaller than that of the stable molecule of similar size, and the difference becomes smaller with increasing the molecular size; (c) The difference of the diffusion constant of the radical from that of the stable molecule is smaller than that observed in the liquid solvent. The property (a) is not unique to the radical diffusion, and the property (b) is the same as is observed in the liquid solvent. The property (c) is most characteristic of the measured density region.

5. Concluding Remarks

We have studied the density dependence of the diffusion constants of the radicals produced by photochemical reactions with TEA in CO_2 and CF_3H . The relatively small difference of the diffusion constants between the radical and the stable molecule in comparison with the difference in the liquid state is the most characteristic feature in the measured density region. To discuss further the origin of this difference between the medium-density region and the liquid densities, we need detailed information how the solute-solvent interaction affects the translational motion of the molecule at each solvent density. To get such information, we are now doing the computer simulation for the system interacting with the Lennard-Jones potential and are studying the effect of the solute-solvent attractive interaction on the solute diffusion. Preliminary results on the computer simulation suggests that the smaller effect of the attractive interaction may be ascribed to the hydrodynamic back flow effect, which is typically seen in the velocity autocorrelation function as a long tail with decaying $t^{-3/2}$.³⁷ The long-time range hydrodynamic correlation diminishes the effect of the solute-solvent attractive interaction. The details of the computer simulation will be published in the near future.³⁸

Acknowledgment. This work is supported by the Research Grant-in-Aid from the Ministry of Education, Science, and Culture (Grant 07640673).

References and Notes

- (1) Terazima, M.; Hirota, N. *J. Chem. Phys.* **1993**, *98*, 6257.
- (2) Terazima, M.; Okamoto, K.; Hirota, N. *J. Phys. Chem.* **1993**, *97*, 13387.
- (3) Terazima, M.; Okamoto, K.; Hirota, N. *J. Chem. Phys.* **1995**, *102*, 2506.
- (4) Okamoto, K.; Terazima, M.; Hirota, N. *J. Chem. Phys.* **1995**, *103*, 10445.
- (5) For example, see: Tyrrel, H. J. V.; Harris, K. R. *Diffusion in Liquids*; Butterworths: London, 1984.
- (6) Okamoto, K.; Terazima, M.; Hirota, N. *J. Phys. Chem.*, submitted for publication.
- (7) Morita, A.; Kato, S. *J. Am. Chem. Soc.*, in press.
- (8) For example, see: Savage, P. E.; Gopalan, S.; Mizan, T. I.; Martino, C. J.; Brock, E. E. *AIChE J.* **1995**, *41*, 1723.
- (9) Kimura, Y.; Yoshimura, Y. *Mol. Phys.* **1991**, *72*, 279.
- (10) For example, see: Funazukuri, T. *Rev. High Pressure Sci. Technol.* **1996**, *5*, 34.
- (11) Liong, K. K.; Wells, P. A.; Foster, N. R. *Ind. Eng. Chem. Res.* **1991**, *30*, 1329.
- (12) Dahmen, N.; Kordikowski, A.; Schneider, G. M. *J. Chromatogr.* **1990**, *505*, 169.
- (13) Feist, R.; Schneider, G. M. *Sep. Sci. Technol.* **1982**, *17*, 261.
- (14) Sassi, P. R.; Mourir, P.; Caude, M. H.; Rosset, R. H. *Anal. Chem.* **1987**, *59*, 1164.
- (15) Funazukuri, T.; Nishimoto, N.; Wakao, N. *Proceedings of the 3rd International Conference of Supercritical Fluids*; Brunner, G.; Perrut, M., Eds. Strasbourg, France, 1994; Tome I, 29.
- (16) Kimura, Y.; Kanda, D.; Terazima, M.; Hirota, N. *Ber. Bunsen-Ges. Phys. Chem.* **1989**, *93*, 791.
- (17) Kimura, Y.; Yoshimura, Y. *J. Chem. Phys.* **1992**, *96*, 3824.
- (18) Huang, F. H.; Li, M. H.; Lee, L. L.; Starling, K. E.; Chung, F. T. *H. J. Chem. Eng. Jpn.* **1985**, *18*, 490.
- (19) Rubio, R. G.; Zollweg, J. A.; Streett, W. B. *Ber. Bunsen-Ges. Phys. Chem.* **1989**, *93*, 791.
- (20) Kimura, Y.; Takebayashi, Y.; Hirota, N. *J. Phys. Chem.* **1996**, *100*, 11009.
- (21) Hayon, E.; Ibata, T.; Lichtin, N. N.; Simic, M. *J. Phys. Chem.* **1972**, *76*, 2072.
- (22) Roberts, C. B.; Zhang, J.; Brennecke, J. F.; Chateaufneuf, J. E. *J. Phys. Chem.* **1993**, *97*, 5618.
- (23) Amada, I.; Yamaji, M.; Sase, M.; Shizuka, H. *J. Chem. Soc., Faraday Trans.* **1995**, *91*, 2751.
- (24) Patel, K. B.; Wilson, R. L. *J. Chem. Soc., Faraday Trans. I* **1973**, *69*, 814.
- (25) Kanda, D.; Kimura, Y.; Terazima, M.; Hirota, N. *Ber. Bunsen-Ges. Phys. Chem.* **1996**, *100*, 656.
- (26) Funazukuri, T.; Ishiwata, Y.; Wakao, N. *AIChE J.* **1992**, *38*, 1761.
- (27) Liong, K. K.; Wells, P. A.; Foster, N. R. *Ind. Eng. Chem. Res.* **1992**, *31*, 390.
- (28) Funazukuri, T.; Hachisu, S.; Wakao, N. *Ind. Eng. Chem. Res.* **1991**, *30*, 1323.
- (29) Reid, R. C.; Prausnitz, J. M.; Poling, B. E. *The Properties of Gases and Liquids*, 4th ed.; McGraw-Hill: New York, 1987.
- (30) LeBas, G. *The Molecular Volumes of Liquid Chemical Compounds*; Longmans, Green: New York, 1915.
- (31) Shenai, V. M.; Hamilton, B. L.; Matthews, M. A. In *Supercritical Fluid Engineering Science*; American Chemical Society: Washington, DC, 1993; Chapter 8.
- (32) Imotov, M. B.; Tsekanskaya, Yu. V. *Russ. J. Phys. Chem.* **1971**, *45*, 744.
- (33) Swaid, I.; Schneider, G. M. *Ber. Bunsen-Ges. Phys. Chem.* **1979**, *83*, 969.
- (34) Lauer, H. H.; McManigill, D.; Board, R. D. *Anal. Chem.* **1983**, *55*, 1370.
- (35) Suarez, J. J.; Bueno, J. L.; Medina, I. *Chem. Eng.* **1993**, *48*, 2419.
- (36) Eckert, C. A.; Ziger, D. H.; Johnston, K. P.; Kim, S. *J. Phys. Chem.* **1986**, *90*, 2738.
- (37) Alder, B. J.; Wainwright, T. E. *Phys. Rev.* **1970**, *A1*, 18. For an example of the detailed discussion on the hydrodynamic effect, see: Boon, J. P.; Yip, S., In *Molecular Hydrodynamics*, McGraw-Hill: New York, 1980; Chapter 3.
- (38) Yamaguchi, T.; Kimura, Y.; Hirota, N., in preparation.